Available online at www.sciencedirect.com
ScienceDirect
Surface & Coatings Technology 201 (2006) 2364–2368
SURFACE & COATINGS TECHNOLOGY
www.elsevier.com/locate/surfcoat

On the formation of periodic segmentation cracks in a coating plated on a substrate with periodic subsurface inclusions

Chen-Wu Wu [a,b], Guang-Nan Chen [a], Kun Zhang [a,*], Ying Hu [a,b], Nai-Gang Liang [a]

[a] *Materials Processing Center, Institute of Mechanics, Chinese Academy of Sciences, No.15 Beisihuanxi Road, Beijing, PR China, (100080)*
[b] *Graduate School of the Chinese Academy of Sciences, Beijing, China*

Received 22 March 2006; accepted in revised form 6 April 2006
Available online 8 June 2006

Abstract

The mechanism of the formation of periodic segmentation cracks of a coating plated on a substrate with periodic subsurface inclusions (PSI) is investigated. The internal stress in coating and subsequently the strain energy release rate (SERR) of the segmentation cracks are computed with finite element method (FEM). And the effect of the geometrical parameters of the PSI is studied. The results indicate that the ratio of the width of the inclusion to the period of the repeated structure has an optimum value, at which the maximum internal tensile stress and SERR arise. On the other hand, the ratio of the max-thickness of the inclusion to the thickness of the coating has a threshold value, above which the further increase of this ratio should seldom influence the internal stress or the SERR.

Keywords: Coating; Periodic subsurface inclusions; Periodic segmentation cracks; Finite element method

1. Introduction

Coatings with resistance to wear, corrosion and thermal degradation are adopted in a great many structures. Unfortunately, the prospective applications of coatings are restricted with its premature spalling. Many designs such as gradient coating, multilayer coating are developed to enhance the durability of coating [1,2]. These designs generally take an intact coating as preference. Recently investigators observed experimentally that the pre-segmentation-cracked coating presents better quality in enduring thermal shock than the initial intact coating [3,4]. It is commonly accepted that those pre-existing segmentation cracks increased the strain tolerance of the coating and thereby, the thermal stresses caused by difference of thermo-mechanical properties between the coating and the substrates were greatly reduced. Computation results show that the interfacial stresses [5] or the extension driving forces of the interface crack [4,6], decrease with increasing the density of the segmentation cracks. Herein the segmentation cracks are those surface cracks running perpendicular to the interface and penetrating a depth comparable to the thickness of coating. Commonly, such segmentation cracks are developed in thermal-sprayed TBC, in which the density and the specific morphology can be controlled by adjusting deposition condition or by post-treatment [7,8].

Zhang et al. [9,10] reported a duplex erosion resistant coating achieved with the steel substrate being discrete quenched prior to chromium coating plating. Such a duplex coating with periodic pre-quenched regions is shown in Fig. 1, in which the specimens have been etched with the solution of nitric acid with ethanol to present the cross section profiles. When the specimen is subjected to tempering, which is required for degassing hydrogen after plating, the anticipated periodic segmentation cracking are observed to locate at the interspaces between two adjacent pre-quenched regions [5,10]. It is noteworthy that, in Fig. 1, the pre-quenching of the upper specimen and the under one are dealt with by Nd: YAG laser and CO_2 gas laser, respectively, to obtain the different sizes of the pre-quenched region [11,12]. The mechanisms of the formation of such periodic segmentation cracks are to be investigated in this study. Furthermore, the effects of the geometrical parameters of the

* Corresponding author. Tel.: +86 10 62547527 3; fax: +86 10 62545533.
E-mail addresses: chenwuwu@imech.ac.cn (C.-W. Wu), kzhang@imech.ac.cn (Kun Zhang).

0257-8972/$ - see front matter © 2006 Elsevier B.V. All rights reserved.
doi:10.1016/j.surfcoat.2006.04.005

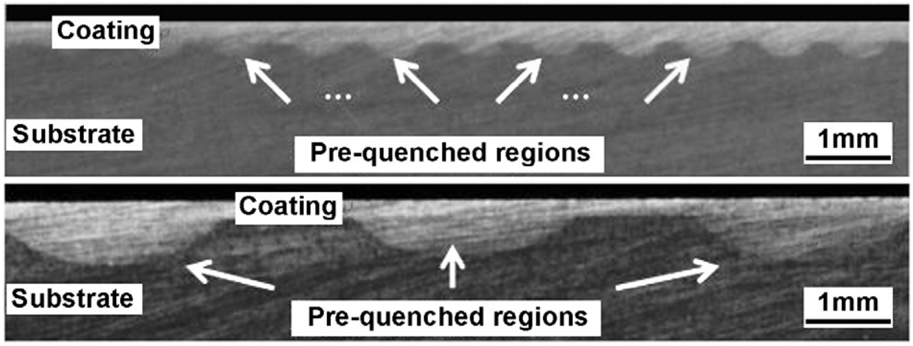

Fig. 1. The cross section profile of the coating and substrate with periodic pre-quenched regions.

pre-quenched regions, namely periodic subsurface inclusion (PSI) as will be introduced in the next section, on the formation of the periodic segmentation cracks are to be studied.

2. Description of the modeling

During tempering the intrinsical volume contractions of the pre-quenched regions will be constrained with the plated coating. Thereby, the system of coating and substrate with Periodic Subsurface Inclusions (PSI) that include eigen-strain are obtained as presented schematically in Fig. 2(a). Herein the definition of the inclusions means that the elasticity of the inclusions is identical to that of the substrate except for the prescribed eigen-strain, for the thorough interpretation of which one is referred to [13]. In Fig. 3, the PSI are denoted by the gray areas, the profile of which is approximated by a circular segment of radius $r=(W_i^2/4+t_i^2)/(2t_i)$, where the symbols W_i and t_i represents the width, the max-thickness of the inclusion and, respectively. And $t_c=0.2$ mm, $t_s=2$ mm, and $W_p=1$ mm represents the thickness of the coating, the thickness the substrate and the period of the repeated structure, respectively. W_t, namely W_p minus W_i, represents the spacing between two adjacent inclusions. L_c denotes the length of the surface crack in coating, namely segmentation crack if L_c is comparable to t_c as aforementioned. The geometrical parameters of the inclusion can be adjusted by altering the power distribution of the laser beam and traverse speed etc [11,12].

In this study, the internal stress in the coating due to the existence of PSI will be computed and the effect of the geometrical parameters of PSI on the internal stress will be investigated. Subsequently, when a surface crack situated at the interspace between two adjacent subsurface inclusions is taken into account as shown in Fig. 2(b), the strain energy release rate is calculated for different geometrical parameters of PSI to study the effect of them on the formation of the segmentation cracking of coating. For simplicity, no other initial stresses, say, that developed during pre-quenching and coating deposition, are included in this study but for the eigen-strain of PSI. At the same time, it is dealt with as a steady-state problem, i.e. no inertial effect is taken into account though the initiation and extension of the surface crack should be of dynamic during tempering.

The assumption of linear elastic plane strain deformation is adopted here, i.e. only the deformations within plane OXY are considered. That is $\varepsilon_x=[\sigma_x-\sigma_y/v]/E$, $\varepsilon_y=[\sigma_y-\sigma_x/v]/E$, and $\varepsilon_z=0$ for both coating and substrate, where ε, σ represents strain and stress, v is Poisson's ratio, E the elastic modulus. Moreover, the periodically symmetry along X-axis of the system is used to decrease the computational work. Thus, only a period of the structure of width W_p is modeled in calculation and the periodically symmetry constraints are exerted on both sides as shown in Fig. 3.

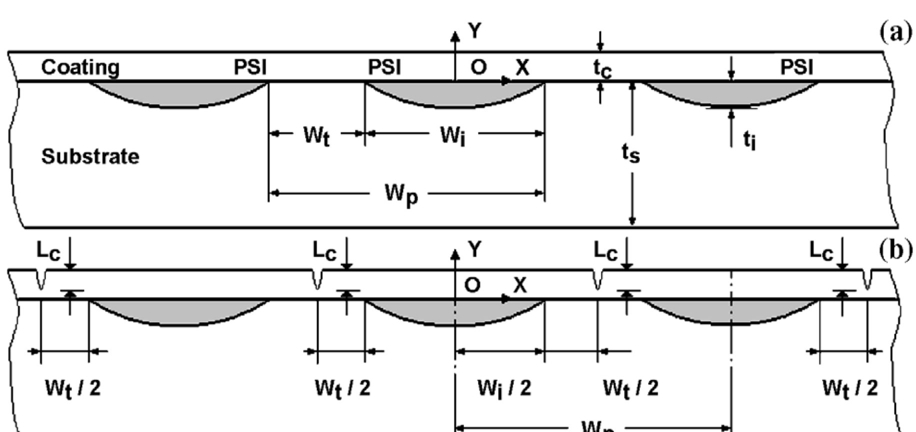

Fig. 2. Schematic of (a) the coating and substrate with PSI and (b) surface crack.

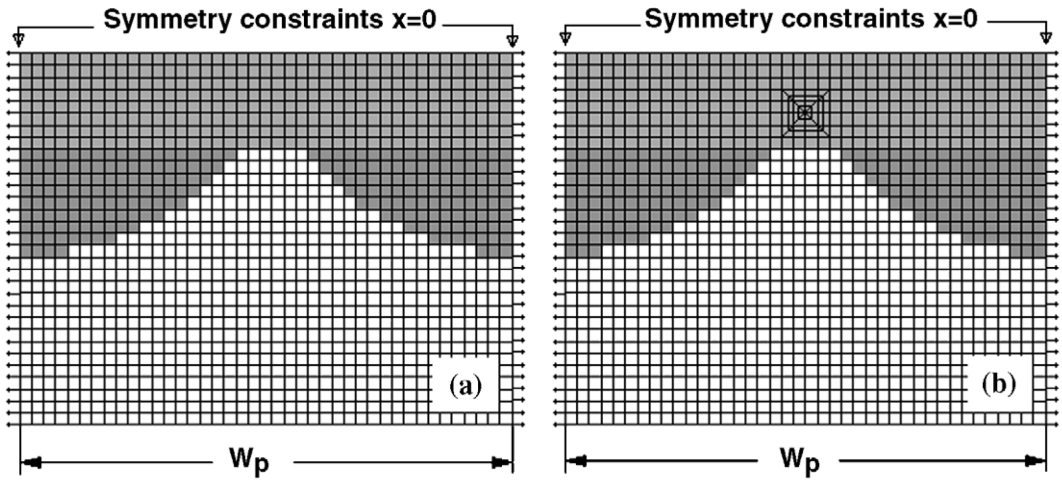

Fig. 3. The schematic of mesh and constraints for the case (a) without and (b) with crack.

Such a complex boundary value problem is solved with the Finite Element Method by ANSYS, of which an 8-nodes quadrilateral element is used and the schematic of the mesh for both the cases without and with surface crack in coating are illustrated in Fig. 3. In Fig. 3(b), around crack tip the mesh are refined with a 6-nodes triangular element to meet the accuracy requirement. The virtual crack extension method [14] is adopted to calculate the Strain Energy Release Rate (SERR) of the body with periodic surface cracks. In the virtual crack extension method, two analyses should be performed, one with crack length a and the other with crack length $a+\Delta a$. The potential energy (strain energy) U per unit thickness for both cases is stored, and the energy release rate can be calculated from

$$\mathrm{SERR} = -\frac{U_{a+\Delta a} - U_a}{1 \times \Delta a}$$

where '1' denotes the unit thickness of the fracture model for plane stain and herein a should be replaced with L_c. The fracture mechanics characterization parameter SERR is determinate even the crack tip approach to the interface [15,16], although wherein the oscillatory singularity is believed to arise due to the existence of the interface between the coating and the substrate.

3. The internal stresses in coating due to the PSI

Fig. 4 illustrates the internal normal stress σ_{xx} for a period in coating, in which the abscissa ranges from the center of an inclusion to that of the adjacent one. Where, $\bar{\sigma} = E \times \bar{\varepsilon}, E = \frac{E_c E_s}{E_c + E_s}, \bar{\varepsilon} = \varepsilon_0, E_c = 300$ GPa, $E_s = 200$ GPa, $\varepsilon_0 = 0.01$ [17,18]. And the ratio of W_i to W_p is 0.8, t_i to t_c is 1.0. The curves in Fig. 4 represent the distribution of the normal stress σ_{xx} corresponding to different y-coordinates, which shows that the portion of coating covered by tensile stress decreases with the increase of the distance apart from the interface. It appears to be induced by the bending effect of the coating, which introduces a non-uniform stress state along the cross section of the coating. Nevertheless, as a whole, the compressive internal stress arises within the coating bonded to the inclusions while tensile internal stress within the coating bonded to the interspaces between two

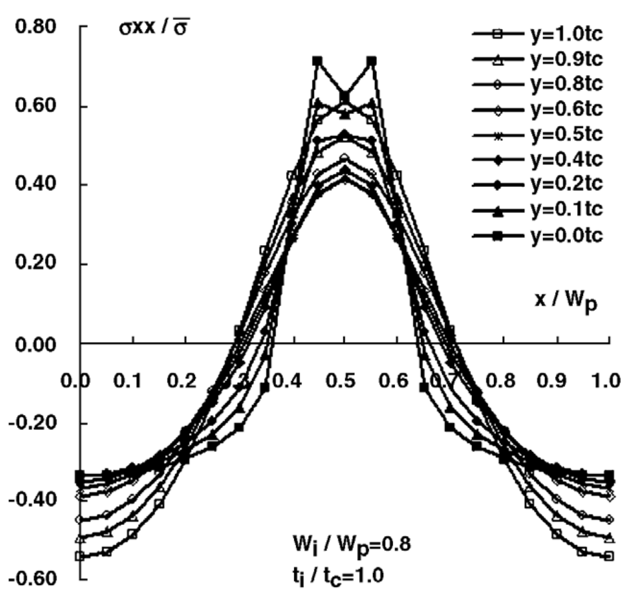

Fig. 4. Internal normal stress σ_{xx} for different y-coordinates in coating.

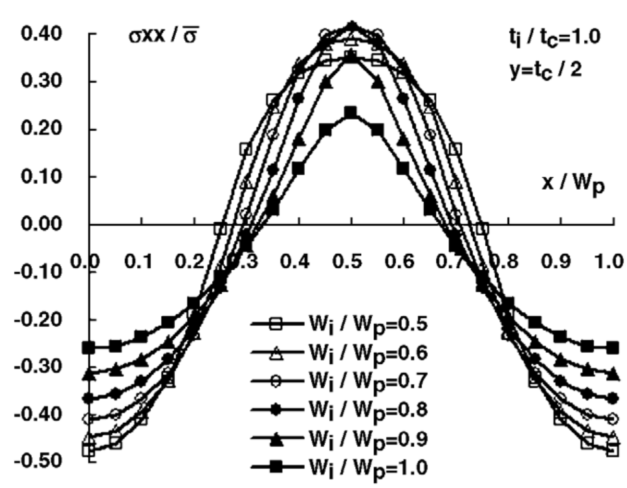

Fig. 5. Internal normal stress σ_{xx} for different value of W_i/W_p.

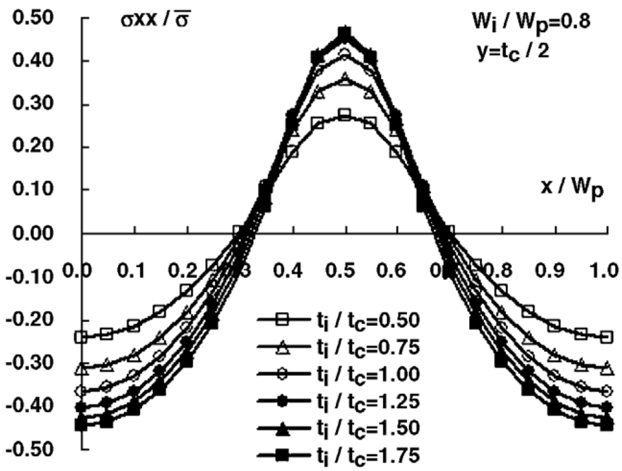

Fig. 6. Internal normal stress σ_{xx} for different t_i/t_c.

adjacent inclusions. Thus, a periodic-altering internal stress in coating is introduced by the PSI. Such periodic-altering internal stress state will lead to the periodic surface cracking, as one can understand that the coating is prone to crack within the region of tensile stress once the maximum tensile stress is above the strength of the material of coating.

The curves in Fig. 5 display the distributions of the stress σ_{xx} in coating of the different ratios of the width of the inclusion (W_i) to that of the period (W_p). Herein the ratio of t_i to t_c is 1. And the path locates at $y=0.5t_c$. It is indicated that the maximum compressive stress decreases with the increase of the ratio of W_i to W_P, i.e. the width fraction of the inclusion in a period. Nevertheless, the peak of the tensile stress increases with the increase of the W_i/W_p before it approaches to the range of 0.7 to 0.8. After the W_i/W_p being over 0.8, the peak of the tensile stress decreases with the increase of the W_i/W_p. Hence, the most acute tensile stress should be obtained in coating if the W_i/W_p falls in the range of 0.7–0.8.

The curves in Fig. 6 show the distribution of the stress σ_{xx} in coating of the different ratios of the thickness of the inclusion to

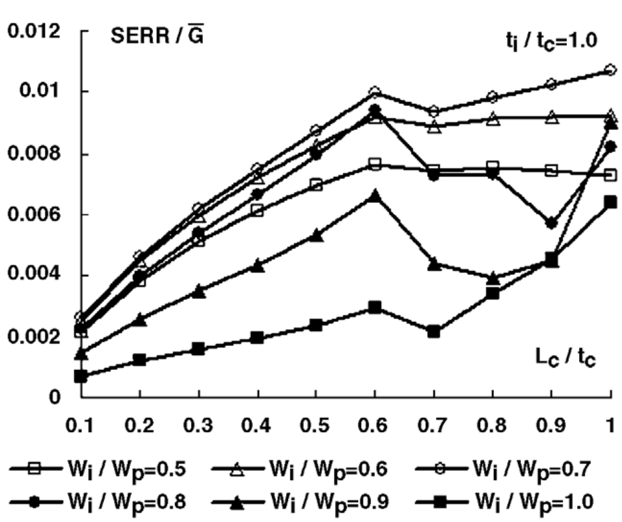

Fig. 7. SERR of surface crack for different W_i/W_p.

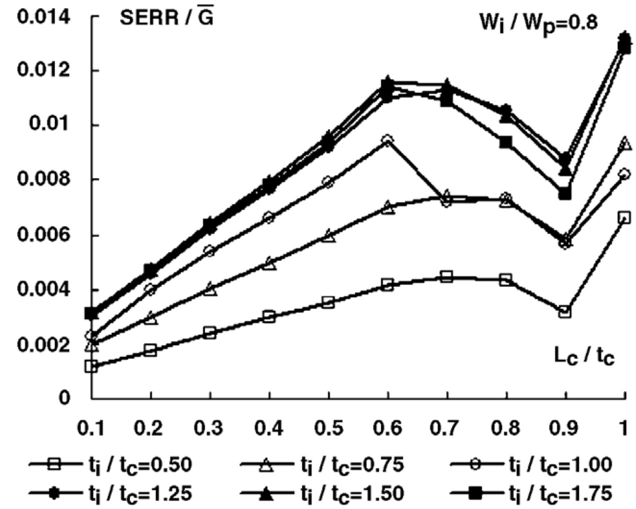

Fig. 8. SERR of surface crack for different t_i/t_c.

that of the coating. Herein the ratio of W_i to W_p is 0.8. Similarly, the path locates at $y=0.5t_c$. It can be found that when increasing the ratio of t_i to t_c, the stress distribution becomes more steep. However, if the t_i/t_c approaches to about 1.5, the variation of the stress distribution is slight, which means the ratio of t_i to t_c also has a threshold as far as only its effect on the stress distribution is considered. This threshold seems to be about 1.5. That is, as soon as the max-thickness of the inclusion approaches to about 1.5 times the thickness of the coating, the tensile stress will not change evidently even increasing the max-thickness of the inclusion.

4. The strain energy release rate of the surface crack due to the PSI

Fig. 7 illustrates the strain energy release rate (SERR) versus the different crack length L_c, in which the different curve is in accord with case with some specific ratio of the width of the inclusion (W_i) to that of the period (W_p). Where, $\bar{G} = \bar{\sigma} \times \frac{t_c \cdot t_c}{t_s}, t_c = 0.2\ \text{mm}, t_s = 1\ \text{mm}$. Herein the ratio of t_i to t_c is 1. One can see that SERR of the prescribed identical surface crack increase with the increase of the ratio W_i/W_p when it is lesser than 0.7. Once W_i/W_p is above that 0.7, the SERR decrease with the increase of the ratio W_i/W_p. This proves again that there exists an optimal value of W_i/W_p as far as its effect on the formation of the segmentation crack is taken into account. And this optimal value is approximately 0.7–0.8.

Fig. 8 illustrates the strain energy release rate (SERR) versus the different crack length L_c for the cases with different ratio of the thickness of the inclusion (t_i) to that of the coating (t_c). Herein the ratio of W_i to W_p is 0.8. The SERR of the prescribed identical surface crack increases with the increase of the ratio t_i/t_c. Again, when the ratio t_i/t_c approaches to about 1.5, the SERR is almost invariable corresponding to the relevant crack length. The threshold of the ratio t_i/t_c is confirmed again as far as its effect on the formation of the segmentation crack is taken into account.

From Figs. 7 and 8, one can find out that, as a whole, the SERR increase with the increase of the crack length L_c. Nevertheless, every curve of SERR versus L_c have its inflexion at about $L_c = 0.6\ t_c$. This indicates that after the crack length is over than 60% of the thickness of coating, the SERR decrease with the increase of the crack length. This may account for the penetration depths of the segmentation cracks. More complications arise in the variation of SERR when the crack tip approaches to the interface, which is believed to be due to the abrupt alteration of materials properties across the interface.

5. Conclusions

Periodic-altering internal stress would arise within the coating due to the existence of the PSI. Such internal stress pattern would lead to the periodic surface crack, which evolved into segmentation crack with penetrating over a depth comparable to the thickness of the coating.

When the surface crack in coating is taken into account, it is found that the SERR increases with the increase of the crack length, as a whole. However, when the crack length exceeds about 60% thickness of the coating, the SERR shows a complex variation with the increase of crack length. This complication is expected to be induced by the abrupt alteration of materials properties in the idealization interface.

The maximum internal tensile stress σ_{xx} in coating or the maximum SERR of the prescribed identical surface crack should exist when the ratio W_i/W_p has some value within the range of 0.7–0.8. Away from this inflexion, increasing or decreasing the ratio W_i/W_p will reduce the maximum of σ_{xx} and SERR of surface crack.

The internal tensile stress σ_{xx} in coating or the SERR of the prescribed identical surface crack increases with the increase of the ratio t_i/t_c, while the influence of whose variation becomes very slight if it is above about 1.5. That is to say, as far as its effect on the σ_{xx} or SERR is considered, the ratio t_i/t_c has a threshold of about 1.5.

Acknowledgement

The financial support provided by the National Natural Science Foundation of China (Grant NO. 50471087, 50531060 and 10572140) is greatly acknowledged.

References

[1] L.L. Shaw, Compos., Part B Eng. 29 (1998) 199.
[2] K. Kokini, J. DeJonge, S. Rangaraj, B. Beardsley, Surf. Coat. Technol. 154 (2002) 223.
[3] Bin Zhou, Klod Kokini, Acta Mater. 52 (2004) 4189.
[4] Bin Zhou, Klod Kokini, Surf. Coat. Technol. 187 (2004) 17.
[5] Chen-Wu Wu, Guang-Nai Chen, Kun Zhang, Geng-Xing Luo, Nai-Gang Liang, Surf. Coat. Technol. xx (2005) xxx-xxx (Available online).
[6] Bin Zhou, Klod Kokini, Mater. Sci. Eng., A 348 (2003) 271.
[7] H.B. Guo, R. Vaßen, D. Stover, Surf. Coat. Technol. 186 (2004) 353.
[8] C. Batista, A. Portinha, R.M. Ribeiro, V. Teixeira, M.F. Costa, C.R. Oliveira, Surf. Coat. Technol. 200 (2006) 2929.
[9] K. Zhang, C.W. Wu, Y. Hu, G.N. Chen, in: I.S. Chung (Ed.), The 3rd Asian Conference on Heat Treatment of Materials, Gyeongiu, (Korea), 2005, p. 216.
[10] Y. Hu, K. Zhang, G.N. Chen, C.W. Wu, Heat Treat. Met. (in Chinese) 30 (2005) 161 (supp.).
[11] Liu Qingbin, Liu Hong, J. Mater. Process. Technol. 88 (1999) 77.
[12] J.C. Ion, Surf. Eng. 18 (2002) 14.
[13] Toshio Mura, Micromechanics of defects in solids, Martinus Nijhoff Publishers, 1982, p. 2.
[14] Ansys: Guidance to structure analysis (v0205) (In Chinese), Ansys. Inc., (2000), p. 6 (Section 4.).
[15] J.W. Hutchinson, Z. Suo, Adv. Appl. Mech. 29 (1992) 63.
[16] W. Yang, Macro and Micro Fracture Mechanics, Chinese National Defence Industry Press, 1995, p. 158, In Chinese.
[17] Z.X. Zhang, Handbook of Enginery Metal materials, Weapon Industry Press, Beijing, 1989, In Chinese.
[18] Z. Liu, Z.J. Wu, J.Z. Wu, Y. Zhang, Numerical Simulation on the Heat Treatment Process, Science Press, Beijing, 1996, In Chinese.